Muñoz-Pina, S.; Ros-Lis, JV.; Argüelles Foix, AL.; Coll, C.; Martínez-Máñez, R.; Andrés Grau, AM. (2018). Full inhibition of enzymatic browning in the presence of thiol-functionalised silica nanomaterial. Food Chemistry. 241:199-205. https://doi.org/10.1016/j.foodchem.2017.08.059

FULL INHIBITION OF ENZYMATIC BROWNING IN THE PRESENCE OF THIOL-FUNCTIONALISED SILICA NANOMATERIAL

Sara Muñoz-Pina[1], José V. Ros-Lis[2]*, Ángel Argüelles[1], Carmen Coll[3,4], Ramón Martínez-Máñez[3,4], Ana Andrés[1]

[1] *Instituto Universitario de Ingeniería de Alimentos para el Desarrollo (IUIAD-UPV). Universitat Politècnica de València Camino de Vera s/n, 46022, Valencia, Spain.*

[2] *Inorganic Chemistry Department, Universitat de València. 46100, Burjassot, Valencia Spain.*

[3] *Instituto Interuniversitario de Investigación de Reconocimiento Molecular y Desarrollo Tecnológico. Universitat Politècnica de València - Universitat de València. Camino de Vera s/n, 46022, Valencia, Spain.*

[4] *CIBER de Bioingeniería, Biomateriales y Nanomedicina (CIBER-BBN).*

*Corresponding author. Email: J.Vicente.Ros@uv.es

ABSTRACT

Darkening processed fruits and vegetables is caused mainly by enzymatic browning through polyphenol oxidase (PPO) action. Accordingly, we explored the potential of four silica-based materials (MCM-41 nanometric size, MCM-41 micrometric size, UVM-7 and aerosil), non-functionalised and functionalised with thiol groups, to inhibit PPO activity in the model system and apple juice. All materials showed relevant performance when immobilising and inhibiting PPO in model systems, and support topology is a main factor for enzyme immobilisation and inhibition. Thiol-containing silica UVM7-SH showed the greatest inactivation, and similar browning values to those

obtained by acidification. The enzyme's kinetic parameters in the presence of UVM-7-SH suggested non-competitive inhibition, which indicated that the material interacted with the enzyme, but beyond the active centre. In real systems, UVM-7-SH completely inhibited enzymatic browning in apple juice (cv. Granny Smith and cv. Golden Delicious) up to 9 days after 5 minutes of contact.

Key words: PPO, tyrosinase, inhibition, UVM-7, thiols, apple juice.

1. INTRODUCTION

Consumer acceptance of new food products depends on their organoleptic properties, with appearance and colour being the most important factors when making buying decisions, especially about fruits and vegetables. Therefore, maintaining food colour during shelf life is a main objective in the food industry given its possible economic impact. The main reason for colour change with fruits and vegetables is known as enzymatic browning, and it has been estimated that this process is responsible for more than 50% of waste (Whitaker & Lee, 1995).

Enzymatic browning is a complex chemical reaction that is divided into several phases, enzymatic hydroxylation, enzymatic oxidation and non-enzymatic polymerisation. The two first steps are catalysed by polyphenol oxidase (PPO). This process transforms phenolic compounds into polymeric structures, which produce the characteristic brown colour (Bello, 2000).

The polyphenol oxidase (PPO) enzyme (EC 1.14.18.1 o EC 1.10.3.1), also known as tyrosinase, catechol oxidase, monophenol oxidase and creolase, has two copper (II) ions, and each is linked to three histidines (type 3 copper enzyme). In nature, the PPO

enzyme can be found in two different forms to catalyse two distinct reactions. In the first reaction, the hydroxylation of mono-phenols generates ortho-phenols, while the enzyme oxidises these ortho-phenols into quinones in the second one. These forms are met-tyrosinase and oxi-tyrosinase, but only oxi-tyrosinase is able to hydroxylate mono-phenols (Sánchez-Ferrer, Neptuno Rodríguez-López, García-Cánovas, & García-Carmona, 1995; Rolff, Schottenheim, Decker, & Tuczek, 2011). The last enzymatic browning process step consists in the non-enzymatic polymerisation of quinones, which gives rise to melanoides (Rouet-Mayer, Ralambosoa, & Philippon, 1990) that are responsible for colour changes.

The main factors that affect food enzymatic browning are: pH, temperature, enzyme activity, quantity of polyphenols, and presence of oxygen (Martínez & Whitaker, 1995). For this reason, processing vegetal foods with large amounts of active PPO and polyphenols involves the risk of enzymatic browning, which causes colour changes and reduces consumer acceptability.

It is important to note that in Europe, and according to FAOSTAT, apple (*Malus Pumila*) is the second fruit in consumption and production terms, and is also one of the most important polyphenol sources in diet. Given their high polyphenols content, apples are one of the fruits most affected by enzymatic browning (Hertog, Hollman, & Katan, 1992). Apples contain several forms of polyphenols, of which chlorogenic acid is the most important given its high concentration in this fruit (Picinelli, Suárez, & Mangas, 1997). Another is L-tyrosine (Rocha & Morais, 2001), which is also found in other foods such as mushrooms and crustaceans, and it provokes the same browning problems as in apples.

72 Over the years, the industry has adopted different chemical and physical strategies to
73 lessen enzymatic browning and to, therefore, reduce fruit and vegetable losses.
74 Traditionally, heat treatment has been used as an enzymatic inactivation method
75 (Williams, Lim, Chen, Pangborn, & Whitaker, 1986). However, this process has many
76 problems since fruits and vegetables have a considerable amount of thermosensitive
77 compounds, such as vitamins (Bomben, Dietrich, Hudson, Hamilton, & Farkas, 1975),
78 carotenoids and anthocyanins (Buckow, Kastell, Terefe, & Versteeg, 2010), which may
79 be affected during treatment. Besides, temperature applications must be fast and
80 enzymatic inhibition must be complete or the browning process accelerates (Toribio &
81 Lozano, 1986).
82 When chemical treatments are applied, acidulants that lower pH, or chelating agents
83 that interact on the active centre of the enzyme, have been used to inactivate PPO
84 (Sapers et al., 1989). Sulphites have also been employed to prevent colour change, but
85 the potential induction of allergenic reactions in consumers has limited their use in
86 food and beverages (Sapers, 1993).
87 Other non-thermal treatments, such as ultrasounds (Abid et al., 2013), CO_2
88 supercritical (Gui et al., 2007), electrical pulses (Ho & Mittal, 1996), high hydrostatic
89 pressure (HHP) (Juarez-Enriquez, Salmeron-Ochoa, Gutierrez-Mendez, Ramaswamy, &
90 Ortega-Rivas, 2015) and ultraviolet light (Müller, Noack, Greiner, Stahl, & Posten,
91 2014) having shown good results to inactivate PPO, they have their limitations, such as
92 high cost and large machinery requirements.
93 From another point of view, nanotechnology is opening up new research areas in
94 several fields, such as medicine and pharmacology (Vallet-Regí, Balas, & Arcos, 2007),
95 and also in the food industry (Pérez-Esteve, Bernardos, Martínez-Máñez, & Barat,

2013). However in the food industry, the use of nanoparticles has focused on developing encapsulated bioactive compounds and designing active packaging, but applications in industrial processes are still scarce. Silica mesoporous materials are nanomaterials that are synthesised by combining surfactant micellar aggregates with reactive silica precursors (Beck et al. 1992). Depending on the surfactant being used, the resultant materials have different structures and pore sizes, which vary between 2 nm and 50 nm. These materials can also be functionalised easily with diverse chemicals groups. Many silica mesoporous materials have been developed in the last 25 years when the M41S family was discovered by a scientist at Mobil Oil (Beck et al., 1992); e.g., MCM-41 is one of the most investigated materials and has a 2D hexagonal structure. UVM-7 is also a mesoporous material that was synthesised at the University of Valencia in 2002 based on the "atrane route" (El Haskouri et al., 2002). This material is characterised by having both intra-particle and inter-particle pores, which provide the material with a large surface area and a stable pore distribution. These features make these supports ideal for hosting and interacting with enzymes (Ispas, Sokolov, & Andreescu, 2009). Nevertheless, the interactions between silica mesoporous materials and polyphenol oxidase have barely been studied as a strategy to avoid enzymatic browning in food systems (Corell Escuin, García-Bennett, Ros-Lis, Argüelles Foix, & Andrés, 2017), with only a partial inhibition in model systems and no tests available in real samples.

The aim of this work is to study interactions between four silica mesoporous materials (MCM-41 nanometric size, MCM-41 micrometric size, UVM-7 and Aerosil 200), and their parent materials functionalised with thiol groups, with the PPO enzyme, to

evaluate their ability to inhibit enzymatic browning in both model systems and apple juice.

2. MATERIALS AND METHODS

2.1. CHEMICALS

Aerosil 200 was purchased from Evonic industries. Mushroom tyrosinase, Dopamine hydrochloride, L-tyrosine, chlorogenic acid, sodium dihydrogen phosphate and disodium hydrogen phosphate were acquired from Sigma-Aldrich, and were used without further purification. Finally, two different varieties of apples (cv. Granny Smith & cv. Golden Delicious), obtained from a local retailer, were used to prepare juice.

2.2. SYNTHESIS AND CHARACTERISATION OF SILICA MATERIALS

Materials were prepared following known procedures. A detailed description of the synthesis of the three mesoporous nanomaterials, the functionalisation with the thiol groups and their characterisation can be found in the Supplementary Material.

Silica materials characterisation was done by low-angle X-ray powder diffraction (XRD) in a Bruker D8 Advance using CuKα radiation. A JEOL –jem-1010 was employed for the transmission electron microscopy (TEM) characterisation. The amount of thiol groups in the four materials was measured by a TGA/SDTA 851e Mettler Toledo (TGA).

The nitrogen adsorption/desorption isotherms were measured in a volumetric adsorption analyser (Micromeritics ASAP 2020) at a liquid nitrogen temperature (-196^{o}C). The Barret-Joyner-Halenda (BJH) model (Barrett, Joyner, & Halenda, 1951) was fitted to estimate pore size distribution and pore volume, while the specific surface area was calculated by the BET model (Brunauer, Emmett, & Teller, 1938) within the

143 low-pressure range. Wall thickness and a_0 cell were calculated from the porosity and
144 XRD data (Neimark, Ravikovitch, Grün, Schüth, & Unger, 1998).
145
146 2.4. ENZYME KINETICS IN MODEL SYSTEMS
147 Mushroom tyrosinase was used to prepare the model systems. Dopamine, L-tyrosine
148 and chlorogenic acid were tested as substrates. In a typical experiment, 1.25 mL of a
149 solution that contained 0.005 to 2.5 mM of substrate in the presence of 10 mM
150 phosphate buffer at pH 5.5 is mixed with 0.25 mL of the enzyme solution (0.14mg/mL-
151 375 U/mL). Absorbance is measured every 20 seconds at 420 nm. Enzyme kinetic
152 studies were performed at 20ºC in duplicate. Solutions at pH 3.5 and 4.5 were also
153 prepared for dopamine.
154 The initial reaction rate was calculated from the slope of the linear part of the
155 absorbance-time curves. The saturation curve was obtained by plotting the reaction
156 rate values *versus* the different substrate concentrations. Since tyrosinase enzymatic
157 reaction follows the Michaelis-Menten equation (Espín et al., 2000), the corresponding
158 kinetic parameters, K_m and V_{max}, were obtained from the Lineweaver-Burk plot (Doran,
159 1998). Afterwards, the catalytic constant (K_{cat}) and the specific constant were
160 calculated from the kinetic parameters for each substrate and pH. A one-way analysis
161 of variance (ANOVA) was applied to determine the influence of the different substrates
162 and the influence of pH in the case of dopamine.
163
164 2.5. STUDY OF ENZYME-MATERIAL INTERACTIONS IN MODEL SYSTEMS
165 In order to determine the nature of the enzyme-material interaction, two types of
166 studies were conducted: enzyme kinetics in the presence of the material and

quantification of enzyme immobilisation. In the kinetic studies, 0.25mL of the enzyme solution (375 U/mL) were added to 1 mL of phosphate buffer 10 mM (pH=4) that contained 1 mg of material. The resulting suspension was stirred for 2 h to ensure that the interactions between the enzyme and the material were as high as possible. Afterwards, 0.25 mL of dopamine 0.12 mM were added and colour enhancement was monitored for 60 minutes by measuring absorbance, after filtration through a 0.45 μm PTFE filter in a JASCO V-630 model at 420. The same experiment was performed in the absence of the material and was used as a reference. Enzymatic browning inhibition can be calculated from absorbance values according to Equation (1), where Abs_0 and Abs_i were the absorbance at 420 in the absence and presence of the material, respectively.

$$\%\, Inhibition = \frac{Abs_0 - Abs_i}{Abs_0} \qquad (1)$$

The kinetic study with UVM-7-SH at pH 4.5 was performed following the same procedure, which was slightly modified since the stock substrate solution changed from 0.5 to 10 mM to obtain the same final concentration as shown above. The inhibition type caused by the UVM-7-SH material was studied with the Lineweaver-Burk plot, and by following the protocol and equations described in De Arraiga, 1979. The free protein concentration was measured by the Bradford method (Bradford, 1976), based on binding the protein to the dye to form a blue complex. As a control, an enzyme solution (375 U/mL) that contained 1 mg/mL of the material in phosphate buffer at pH=3.5 was used. The calibration line was formed with bovine serum albumin. Absorbance measures were taken with a JASCO model V-630 at 595 nm using 2-mL plastic spectrophotometer cuvettes. Both, the kinetic studies and the Bradford method were run in triplicate

191

192 2.6. MATERIAL TESTING IN APPLE JUICE

193 Apple juice was used as a real food system to test the material selected in the kinetic
194 studies. The test was run on liquefied apples, obtained in the laboratory from two
195 varieties of apple, cv. Granny Smith and cv. Golden Delicious. Three apple juice
196 aliquots of 2 mL were taken from each variety. One of each was combined with 20 mg
197 of either UVM-7 or UVM-7-SH, and the other one was used as the control sample.
198 These mixtures were stirred at 200 rpm for 60 minutes. Colour changes were followed
199 by taking photographs of apple samples.

200 Furthermore, in order to test browning inhibition persistence after removing the
201 material, 4 mL of Golden Delicious juice were placed so they came into contact with 40
202 mg of UVM-7-SH and were stirred for 5 min. Afterwards, the sample was filtered off
203 and the filtrate was separated in two aliquots. One was kept at room temperature and
204 the other one was placed in the refrigerator. Moreover, a sample without the material
205 was used as the control.

206

207 **3. RESULTS AND DISCUSSION**

208 3.1. MATERIALS CHARACTERISATION AND SELECTION

209 Eight materials were prepared as potential inhibitors of PPO. They involved the
210 combination of four supports (MCM-41 micro, MCM-41 nano, UVM-7 and Aerosil 200)
211 with two functionalities: silanols (naturally present on the surface of silica materials),
212 or thiol groups (which were covalently attached to the material's surface). Mesoporous
213 materials have shown the ability to immobilise PPO up to 30% upon enzyme loading
214 (Corell Escuin et al, 2017). The pore size and pore volume of the materials appeared to

215 be the most relevant factor when immobilising PPO. Therefore, a variety of particle
216 size and topologies were selected. MCM-41 and UVM-7 are characterised by an
217 ordered mesoporous bidimensional structure, with a pore diameter of a few
218 nanometers. With MCM-41, two kinds of supports with diverse particle sizes (MCM-
219 41-micro and MCM-41-nano) were prepared to study the effect of particle size on the
220 nanomaterial-enzyme interaction. UVM-7 is a bimodal porous silica material made
221 from the aggregatinon of pseudo-spherical mesoporous nanoparticles (12–17 nm)
222 developing intra-nanoparticles pores (mesopore) of 2–4 nm (a pseudo-hexagonal
223 disordered array) and 20–70 nm inter-particle macro pores (textural porosity) that
224 improve diffusion (El Haskouri el al., 2002). Finally, Aerosil is characterised by the
225 absence of the mesoporous system, although a certain porosity can be observed
226 between particles (textural porosity).
227 The silica supports were covalently modified with thiol groups (-SH). This modification
228 was inspired by the knowledge that cysteine is a well-known PPO inhibitor, and the
229 thiol group in cysteine is the active moiety (Richard-Forget, Goupy, & Nicolas, 1992;
230 İyidoğan & Bayındırlı, 2004). The use of covalent bonding offers greater stability to
231 final systems compared with other possibilities, such as occlusion or electrostatic
232 interactions.
233 X-ray powder diffraction and TEM confirmed that the mesoporous structure was
234 maintained during calcination (while preparing the unfunctionalised materials) and
235 during the functionalisation of the materials with thiols (see the Supplementary
236 Material). The BET analysis of the N_2 adsorption/desorption isotherms offered specific
237 surface values for all the materials that came close to 1,000 m^2g^{-1} after calcination (see
238 Table 1). The specific surface value of the materials functionalised with thiols groups

239 was strikingly similar to the unfunctionalised ones because the thiol chain is not long
240 enough to stop N_2 from entering pores. This tendency was also observed when the BJH
241 model was applied to calculate the specific pore volume of all the solids. In all cases
242 values of around 0.6-0.8 m^3g^{-1} were obtained for the specific mesopore volume in the
243 calcined and functionalised particles. In addition, the calculated pore diameter values
244 were 2.69 nm for UVM-7 and 2.58 for UVM-7-SH. With MCM-14, the calculated pore
245 diameter values were about 2.5 nm for MCM-41 nano and 2.3 for MCM-41 micro for
246 both the unfunctionalised and functionalised supports. As the Aerosil structure does
247 not present mesopores, the only calculated parameter was surface (195.92 m^2g^{-1} for
248 Aerosil and 181.78 m^2g^{-1} for Aerosil-SH). As we can see, the specific surface for Aerosil
249 is much lower than that found for the other supports as its structure lacks mesopores
250 (see Table 1).
251 In addition to mesopores, the materials can also show textural porosity due to the
252 aggregation of smaller sized particles. As observed in Table 1, the prepared supports
253 present textural porosity with pore diameters that fall within the range of 15 nm
254 (MCM-41-nano and Aerosil) or 40 nm (UVM-7), as well as specific textural pore
255 volumes from 0.11 to 1.0 $cm^3\ g^{-1}$.
256 Lastly, the amount of the thiol group present in the mesoporous materials was
257 estimated by a TGA analysis (see Table 1). Values of 0.32, 0.55, 0.75 and 0.54 mmol of
258 thiol/g SiO_2 for Aerosil-SH, MCM41-micro-SH, MCM-41-nano-SH and UVM-7-SH were
259 respectively found. These results fall in line with the expected degree of
260 functionalisation for the silica materials (Ros-Lis et al., 2008). It seems that the smaller
261 specific surface of Aerosil allowed a lower degree of functionalisation, which resulted
262 in the smallest amount of thiol. For the mesoporous materials, which have larger

surfaces, thiol functionalisation increased from 70% (MCM-41-micro and UVM-7) to 140% (MCM-41-nano) compared with Aerosil.

3.2. ENZYME KINETICS IN MODEL SYSTEMS

As pH in fruits and their resultant juices usually ranges from 3.5 to 5.5, the PPO kinetics was measured within this interval. Three substrates that are typically found in the literature for PPO (dopamine, chlorogenic acid and tyrosine) were studied. Among the different substrates, dopamine was clearly the substrate with the greatest enzymatic activity since L-tyrosine and chlorogenic acid had a lower V_{max} (Table 2). In both cases, the turnover number was lower than that for dopamine; however, with chlorogenic acid, affinity was almost as high as it was for dopamine. All the constants statistically differed from one another, with a 99.95% probability. Therefore, dopamine was selected for the other experiments as it exhibited the most intense response.

pH is one of the most relevant parameters to affect biological processes (e.g., enzymatic activity) both in food systems and during food processing. The results in Table 2 show enzyme activity evolution with pH (from 3.5 to 5.5), with almost no activity at pH 3.5. Munjal and Sawhney reported similar results in 2002. With the enzyme-dopamine model system, V_{max}, K_{cat} and the specific constant parameters increased with pH ($p<0.05$), but no significant differences were found for K_m ($p<0.05$). The affinity of the enzyme for dopamine (K_{cat}/K_m) reached values above 3,800 $\Delta Abs_{420} min^{-1} mM^{-1}$ at pH 5.5, which came close to 40 $\Delta Abs_{420} min^{-1} mM^{-1}$ at pH 3.5. Thus a pH of around 4.5 was selected for the assays run in the presence of the materials.

3.3. THE MATERIAL-ENZYME INTERACTION

287 The material-enzyme interaction was studied by analysing PPO activity inhibition in the
288 presence of the eight prepared materials (four supports, with and without thiols).
289 Enzyme activity was quantified through the browning measured at 420 nm 1 hour after
290 adding the substrate to the enzyme solution, with or without the material. All the
291 tested materials, even those non-functionalised with thiols, were able to inhibit
292 enzymatic activity to a certain extent, and went from 19% to 58% (Fig. 1).
293 For the calcined materials, which are covered with silanol groups, inhibitory power
294 decreased in this order: UVM-7 > Aerosil > MCM-41-nano > MCM-41-micro. After
295 taking their structure into account (Table 1), it can be concluded that neither surface
296 nor mesopore volume is a relevant characteristic for enzyme inactivation. The
297 influence of the mesopore diameter could not be ruled out since UVM-7 had wider
298 pores, followed by MCM-41-nano and MCM-41 micro. However, the pore size
299 differences between them were relatively small, and they did not exist in Aerosil,
300 which proved more active than the MCM-41-based materials. So although mesopores
301 seemed to be responsible for certain browning inhibition, they were not the main
302 driver.
303 Presence of textural pores is probably the main structural factor responsible for the
304 differences noted in enzyme activity inhibition between materials. As we can see in
305 Table 1, it seems that an increase in either the textural pore diameter or the textural
306 pore volume enhances inhibitory power. The migration of the enzyme to the material
307 is a diffusion-controlled process (Corell Escuin, García-Bennett, Ros-Lis, Argüelles Foix,
308 & Andrés, 2017), and the smaller the pore diameter, the more difficult it is for the
309 enzyme to enter pores, particularly pores below 3 nm. The experimental results
310 suggested that the enzyme was able to interact with mesopores, but a combined

311 interaction with mesopores and textural pores was probably the most effective
312 approach to inactivate it.
313 When the materials were functionalised with thiols, PPO inhibition increased with
314 values between 29% for MCM-41-micro-SH and 58% for UVM-7-SH (Figure 1). The
315 inhibitory effect of the diverse materials followed the same order as that found for the
316 calcined materials, but the additional effect accomplished by thiol groups differed
317 depending on the support type. While inhibition respectively increased by 12.2%,
318 11.15 and 10.1% for UVM-7-SH, MCM-41-nano-SH and MCM-41-micro-SH compared
319 to the calcined material, this increment with Aerosil was only 4%. It would appear that
320 thiol functionalisation improved PPO inhibition in particular materials which contained
321 mesopores, and then induced a similar increase for all three materials. On the contrary
322 for Aerosil, the effect of the material without mesopores was significantly weaker
323 ($p<0.01$).
324 It is feasible to think that the weaker effect of thiol in Aerosil could be attributed to its
325 lower thiol loading compared to the mesoporous supported materials. However, a
326 regression coefficient (R^2) as low as 0.0023 was obtained for the other three materials
327 when we performed a correlation after removing Aerosil-SH, which refutes such a
328 hypothesis. Therefore, the results suggested that UVM-7-SH was the material with the
329 strongest inhibitory power due to the synergetic effect of the bimodal pore system
330 with the strong effect of thiols.
331 In order to gain further insight into the inhibition mechanism, the amount of enzyme
332 captured by the material was determined indirectly by quantifying the amount of free
333 enzyme present in the solution by the Bradford method. The results showed that 2 h
334 after coming into contact with 1 mg of the material, the percentage of immobilised

335 enzyme fell within the 50-71% range (Fig. 2). In this case, the type of material also
336 affected the % of immobilised enzyme, but these differences were narrower than for
337 enzymatic activity. Furthermore, the thiol groups improved enzyme immobilisation,
338 and this effect was observed only in those materials that contained mesopores.
339 However, an unsatisfactory correlation was found among the concentration of thiols
340 and the increase of the enzyme immobilization (R^2 = 0.211).
341 The percentage of immobilised enzyme was higher than the reduced activity for all the
342 tested materials. This suggests that part of the immobilised enzyme maintains its
343 activity or immobilisation induces only partial inhibition. Furthermore, the thiol groups
344 enhanced both the inhibitory potential and the immobilisation percentage.
345
346 3.4. THE TYROSINASE-UVM-7-SH INTERACTION
347 Since UVM-7-SH offered the best performance in overall PPO activity reduction and
348 the highest percentage of inhibition for the immobilised enzyme, a kinetic study was
349 performed at pH 4.5. The aim of this set of experiments was to compare the results
350 with the previous results obtained in Section 3.2, and to understand the type of
351 inhibition by using the Lineweaver–Burk plot. As expected, the reaction rate V_{max} was
352 much lower in the presence of 1 mg of UVM-7-SH than that at the same pH without
353 the material. A slight reduction in enzyme affinity was also observed (K_m) for the
354 substrate (Table 2). In the presence of UVM-7-SH, both the turnover number (K_{cat}) and
355 catalytic efficiency (K_{cat}/K_m) of the enzyme plummeted from values near 2,500 to some
356 of around 40 for both constants. These findings indicated that enzyme activity
357 significantly decreased in the presence of UVM-7-SH. It was also noted that these
358 values were similar to those obtained for the enzyme at pH 3.5, which demonstrated

359 that UVM-7 functionalised with thiol groups caused a similar enzyme inhibition to that
360 accomplished by an acidic pH. This indicates a clear advantage of using UVM-7 to
361 control enzyme activity instead of the acidification strategy as the sensorial properties
362 of the food system remain unaltered.
363 The K_m and V_{max} values suggested that the inhibition mechanism was non-competitive
364 as no statistically significant differences were observed for K_m, while V_{max} lowered. This
365 result indicated that although the UVM-7-SH-enzyme interaction did not occur in the
366 substrate active centre, it seemed to modify the interaction between the substrate and
367 the active centre by stopping the product formation reaction (Harvey & Ferrier, 2011).
368 As the final objective of obtaining a PPO inhibitor material was to avoid enzymatic
369 browning in fruit juice, the material-enzyme ratio was tested at pH 4.5 and 5.5. No test
370 was performed at pH 3.5 as activity at this pH was too low and it was difficult to
371 spectrophotometrically follow inhibition. As the enzyme was more active at pH 5.5
372 than it was at pH 4.5, and in order to facilitate interpretation, the results are shown as
373 a percentage of inhibition, and refer to the control at the corresponding pH.
374 UVM-7-SH was unable to prevent browning when used at low concentrations (0.3 and
375 1 mg of the material), and concentrations above 3 mg were needed to inhibit the
376 generation of brown pigments (see Fig. 3). Similar results were obtained for the two
377 pH conditions, which suggests that inhibition does not depend on the pH of the
378 solution, at least not for the studied interval. The pKa of the thiol groups (pKa $\cong$10) was
379 far from the pH of the trials, and no relevant change in the material's surface
380 properties was expected between pH 4.5 and 5.5.
381 The influence of the substrate on the material-enzyme interaction was also tested. For
382 this purpose, L-tyrosine and chlorogenic acid were used as substrates instead of

dopamine, and a similar response was observed (see supplementary material). Increasing the quantity of UVM-7-SH in the model system enhanced inhibition, and total inhibition was accomplished with 3 mg per 93.75 U. The results suggest that the material's capacity to inhibit enzyme activity is independent of the substrate and pH, and the material-enzyme ratio is the only critical variable for the inhibition process.

Lastly, it should be considered that the enzyme and substrate would be present in the same matrix in a real application. Therefore, the enzymatic reaction will start as soon as cellular content is exposed to oxygen. Thus it is advisable that the material is able to interact with the enzyme as quickly as possible, ideally no sooner than the material is added. In order to evaluate the requirement of the contact time between the enzyme and the material, diverse contact times were tested before adding the substrate (0, 1, 10 min and 2 h). The assay was performed at pH 4.5 at a 3 mg/93.75 U ratio since these were the conditions at which full enzyme inhibition was achieved. The obtained results showed that the previous contact time only had a minor effect on the material response, and 97% inhibition was achieved in short times, with 100% inhibition for longer times.

The results confirmed that combining the UVM-7 structure with thiol groups was able to empower inhibition, and up to a point at which enzymatic browning was no longer significant. This scenario suggests that a suitable UVM-7-SH:enzyme ratio could stop enzymatic reactions and could, therefore, avoid enzymatic browning in real food systems.

3.6. UVM-7-SH PERFORMANCE IN APPLE JUICE

406 Once the good response of UVM-7-SH particles had been proved in model systems, the
407 effect of mesoporous particles on real juice was studied. Two apple varieties were
408 chosen for the test. Golden Delicious was chosen as this is the most widely consumed
409 cultivated variety in Europe. Granny Smith was selected for its homogeneous
410 composition between different batches and origins, which guarantees reproducibility
411 in the results (Barrera, Betoret, Corell, & Fito, 2009).
412 Diverse UVM-7-SH concentrations were added to the fresh liquefied apple juice. The
413 results showed that 1 mg/mL of the material added to apple juice was insufficient to
414 stop enzymatic browning. When the concentration was increased to 5 mg/mL, the
415 browning reaction was delayed and progressed similarly to the control after 10
416 minutes. The addition of 10 mg/mL to both varieties led to the total PPO enzyme
417 inhibition of juice samples. According to the literature (Reinkensmeier et al., 2016), the
418 enzymatic activity in both apple varieties was similar, which explains why the same
419 amount of mesoporous material was needed to ensure inhibition for both varieties.
420 Besides, these outputs suggested a direct dependency between the UVM-7-SH
421 concentration and PPO enzyme activity.
422 Persistence of inhibition is shown in Figure 4a and 4b; the vials on the left contain
423 natural apple juice with no added material, while those on the right contain 10 mg/mL
424 of UVM-7-SH. The enzymatic browning process, which is characteristic of fresh apple
425 juice, is observed in the samples on the left. Colour change was observed in early
426 stages (under 1 minute) due to the speed of the oxidation process. After a 5-minute
427 exposure to oxygen, juice became red-copper, which vastly differed from its original
428 yellow colour. However, no enzymatic browning was observed in these fresh juice
429 samples when the UVM-7-SH material was added. The inhibiting effect of the

mesoporous material was strong enough to completely stop the process; as we can see, the juices without the material had completely oxidised after 60 minutes.

The same test was performed, but UVM-7 was used to check the effect of the thiol groups present in the functionalised particles of UVM-7-SH. In this case, enzymatic browning was slightly slowed down by the presence of UVM-7 during the first minutes. A few minutes later, the oxidation process progressed to an advanced stage, even at high concentrations of the material (10 mg/mL) (see supplementary material). This observation evidences that the –SH groups are essential for developing enzyme inhibition, and therefore for avoiding enzymatic browning.

A last experiment was carried out by removing the UVM-7-SH from real juice after a 5-minute contact step. The aim of this trial was to explore the possibility of recovering the material and then obtaining a final juice free of particles. After removing the material, two sets of samples were stored at 4°C (Fig. 4c) and at room temperature (20°C) (Fig. 4d). The browning of the refrigerated samples was monitored for 30 days. while the samples stored at room temperature were thrown away after 4 days due to mould growth. We can observe how the freshly filtered sample, previously treated with UVM-7-SH, became colourless and slightly darkened (almost imperceptible to the naked eye) throughout the experiment. As the control sample, a juice solution without the material, but also filtered after being stirred for 5 minutes, was prepared. It was already orange after the 5-minute step, and darkened with time. Therefore, it can be stated that the UVM-7-SH material has the functionality of inhibiting browning and does not need to remain in the system since inhibition endures, and even after it has been removed from an early stage.

4. CONCLUSIONS

It has been demonstrated that mesoporous materials are good candidates to immobilise and inhibit PPO. The effect on the enzyme is dependent on not only the material's structure, but also on functionalisation. It would appear that the mesopores and micropores combination (observed in materials such as UVM-7), together with thiol groups, offers the best inhibitory properties. UVM-7-SH is capable of inhibiting the PPO enzyme and, therefore, of stopping the enzymatic oxidation process when used at concentrations that equal or exceed 3 mg of UVM-7-SH per 93.75 enzymatic units, and does not seem to depend on the substrate. The experiments were performed in both model systems and fresh apple juice, obtained from the Golden Delicious and Granny Smith varieties. Enzymatic browning inhibition in juices remained up to 30 days, even after the material was removed by filtration after a contact stage that lasted only 5 minutes.

AKCNOWLEDEGMENTS

The authors thank the financial support obtained from the Spanish Government (Project MAT2015-64139-C4-1-R) and the Generalitat Valenciana (Project GVA/2014/13).

REFERENCES

Abid, M., Jabbar, S., Wu, T., Hashim, M. M., Hu, B., Lei, S., Zhang, X., & Zeng, X. (2013). Effect of ultrasound on different quality parameters of apple juice. *Ultrasonics Sonochemistry*, *20(5)*, 1182–1187.

478 Barrera, C., Betoret, N., Corell, P., & Fito, P. (2009). Effect of osmotic dehydration on
479 the stabilization of calcium-fortified apple slices (var. Granny Smith): Influence of
480 operating variables on process kinetics and compositional changes. *Journal of Food*
481 *Engineering*, *92(4)*, 416–424.
482 Barrett, E. P., Joyner, L. G., & Halenda, P. P. (1951). The Determination of pore volume
483 and area distributions in porous substances. I. Computations from nitrogen isotherms.
484 *Journal of the American Chemical Society*, *73(1)*, 373–380.
485 Beck, J. S., Vartuli, J. C., Roth, W. J., Leonowicz, M. E., Kresge, C. T., Schmitt, K. D., Chu,
486 C. T. W., Olson, D. H., Sheppard, E. W., McCullen, S. B., Higgins, J. B., & Schlenker, J. L.
487 (1992). A new family of mesoporous molecular sieves prepared with liquid crystal
488 templates. *Journal of the American Chemical Society*, *114(27)*, 10834-10843.
489 Bello Gutierrez, J. (2000). Ciencia bromatológica: principios generales de los alimentos.
490 (1st ed.). Díaz de Santos, 323-334.
491 Bomben, J. L., Dietrich, W. C., Hudson, J. S., Hamilton, H. K., & Farkas, O. F. (1975).
492 Yields and solids loss in steam blanching cooling and freezing vegetables. *Journal of*
493 *Food Science*, *40(4),* 660–664.
494 Bradford, M. M. (1976). A rapid and sensitive method for the quantitation of
495 microgram quantities of protein utilizing the principle of protein-dye binding.
496 *Analytical Biochemistry*, *72(1),* 248-254.
497 Brunauer, S., Emmett, P. H., & Teller, E. (1938). Adsorption of gases in multimolecular
498 layers. *Journal of the American Chemical Society*, *60(2)*, 309-319.
499 Buckow, R., Kastell, A., Terefe, N. S., & Versteeg, C. (2010). Pressure and temperature
500 effects on degradation kinetics and storage stability of total anthocyanins in blueberry
501 juice. *Journal of Agricultural and Food Chemistry*, *58(18)*, 10076-10084.

Corell Escuin, P., García-Bennett, A., Ros-Lis, J. V., Argüelles Foix, A., & Andrés, A. (2017). Application of mesoporous silica materials for the immobilization of polyphenol oxidase. *Food Chemistry*, *217*, 360-363.

De Arriaga, M. D. (1979). *Cinética enzimática: manejo de datos*. (1st ed.). Universidad de Oviedo. (Chapter 3)

Doran, P. (1998). *Principios de ingeniería de los bioprocesos*. (1st ed.). Acribia: Zaragoza, (Chapter 11).

El Haskouri, J., Zarate, D. O. de, Guillem, C., Latorre, J., Caldes, M., Beltran, A., Beltran, D., Descalzo, A. B., Rodriguez-Lopez, G., Martinez-Manez, R., Marcos, M. D., & Amoros, P. (2002). Silica-based powders and monoliths with bimodal pore systems. *Chemical Communications*, *4*, 330–331

Espín, J. C., Varón, R., Fenoll, L. G., Gilabert, M. A., García-Ruíz, P. A., Tudela, J., & García-Cánovas, F. (2000). Kinetic characterization of the substrate specificity and mechanism of mushroom tyrosinase. *European Journal of Biochemistry*, *267(5)*, 1270–1279.

Gui, F., Wu, J., Chen, F., Liao, X., Hu, X., Zhang, Z., & Wang, Z. (2007). Inactivation of polyphenol oxidases in cloudy apple juice exposed to supercritical carbon dioxide. *Food Chemistry*, *100(4)*, 1678–1685.

Harvey, R. A., & Ferrier, D. R. (2011). *Biochemistry*. (5th ed.). Wolters Kluwer Health/Lippincott Williams & Wilkins, (Chapter 5).

Hertog, M. G. L., Hollman, P. C. H., & Katan, M. B. (1992). Content of potentially anticarcinogenic flavonoids of 28 vegetables and 9 fruits commonly consumed in the Netherlands. *Journal of Agricultural and Food Chemistry*, *40(12)*, 2379–2383.

525 Ho, S. Y., & Mittal, G. S. (1996). Electroporation of Cell Membranes: a review. *Critical*
526 *Reviews in Biotechnology*, *16(4)*, 349–362.
527 Ispas, C., Sokolov, I., & Andreescu, S. (2009). Enzyme-functionalized mesoporous silica
528 for bioanalytical applications. *Analytical and Bioanalytical Chemistry*, *393(2)*, 543-554.
529 İyidoğan, N. F., & Bayındırlı, A. (2004). Effect of l-cysteine, kojic acid and 4-
530 hexylresorcinol combination on inhibition of enzymatic browning in Amasya apple
531 juice. *Journal of Food Engineering*, *62(3)*, 299-304.
532 Juarez-Enriquez, E., Salmeron-Ochoa, I., Gutierrez-Mendez, N., Ramaswamy, H. S., &
533 Ortega-Rivas, E. (2015). Shelf life studies on apple juice pasteurised by ultrahigh
534 hydrostatic pressure. *LWT - Food Science and Technology*, *62(1, Part 2)*, 915–919.
535 Martinez, M. V., & Whitaker, J. R. (1995). The biochemistry and control of enzymatic
536 browning. *Trends in Food Science & Technology*, *6(6)*, 195–200.
537 Müller, A., Noack, L., Greiner, R., Stahl, M. R., & Posten, C. (2014). Effect of UV-C and
538 UV-B treatment on polyphenol oxidase activity and shelf life of apple and grape juices.
539 *Innovative Food Science & Emerging Technologies*, *26*, 498–504.
540 Munjal, N., & Sawhney, S. K. (2002). Stability and properties of mushroom tyrosinase
541 entrapped in alginate, polyacrylamide and gelatin gels. *Enzyme and Microbial*
542 *Technology*, *30(5)*, 613–619.
543 Neimark, A. V, Ravikovitch, P. I., Grün, M., Schüth, F., & Unger, K. K. (1998). Pore size
544 analysis of MCM-41 type adsorbents by means of nitrogen and argon adsorption.
545 *Journal of Colloid and Interface Science*, *207(1)*, 159–169.
546 Pérez-Esteve, E., Bernardos, A., Martínez-Máñez, R., & Barat, J. M. (2013).
547 Nanotechnology in the development of novel functional foods or their package. An

548 overview based in patent analysis. *Recent Patents on Food, Nutrition & Agriculture*,
549 *5(1)*, 35–43.
550 Picinelli, A., Suárez, B., & Mangas, J. J. (1997). Analysis of polyphenols in apple
551 products. *Zeitschrift für Lebensmitteluntersuchung und -Forschung* A, *204(1)*, 48–51.
552 Reinkensmeier, A., Steinbrenner, K., Homann, T., Bußler, S., Rohn, S., & Rawel, H. M.
553 (2016). Monitoring the apple polyphenol oxidase-modulated adduct formation of
554 phenolic and amino compounds. *Food Chemistry*, *194*, 76–85.
555 Richard-Forget, F. C., Goupy, P. M., & Nicolas, J. J. (1992). Cysteine as an inhibitor of
556 enzymic browning. 2. Kinetic studies. *Journal of Agricultural and Food Chemistry*,
557 *40(11)*, 2108–2113.
558 Rocha, A. M. C. N., & Morais, A. M. M. B. (2001). Characterization of
559 polyphenoloxidase (PPO) extracted from "Jonagored" apple. *Food Control*, *12(2)*, 85–
560 90.
561 Rolff, M., Schottenheim, J., Decker, H., & Tuczek, F. (2011). Copper-O_2 reactivity of
562 tyrosinase models towards external monophenolic substrates: molecular mechanism
563 and comparison with the enzyme. *Chemical Society Reviews*, *40(7)*, 4077–4098.
564 Ros-Lis, J. V., Casasús, R., Comes, M., Coll, C., Marcos, M. D., Martínez-Máñez, R.,
565 Sancenón, F., Soto, J., Amorós, P., El Haskouri J., Garró, N., & Rurack, K. (2008). A
566 Mesoporous 3D hybrid material with dual functionality for Hg^{2+} detection and
567 adsorption. *Chemistry - A European Journal*, *14(27)*, 8267–8278.
568 Rouet-Mayer, M.-A., Ralambosoa, J., & Philippon, J. (1990). Roles of o-quinones and
569 their polymers in the enzymic browning of apples. *Phytochemistry, 29(2)*, 435–440.

570 Sánchez-Ferrer, Á., Neptuno Rodríguez-López, J., García-Cánovas, F., & García-
571 Carmona, F. (1995). Tyrosinase: a comprehensive review of its mechanism. *Biochimica*
572 *et Biophysica Acta (BBA) - Protein Structure and Molecular Enzymology*, *1247(1)*, 1–11.
573 Sapers, G. M. (1993). Browning of foods: control by sulfites, antioxidants, and others
574 means. *Food Technology*, *47(10)*, 75-84
575 Sapers, G. M., Hicks, K. B., Phillips, J. G., Garzarella, L., Pondish, D. L., Matulaitis, R. M.,
576 McCormack, T. J., Sondey, S. M., Seib, P. A., & Ei-Atawy, Y. S. (1989). Control of
577 enzymatic browning in apple with ascorbic acid derivatives, polyphenol oxidase
578 inhibitors, and complexing agents. *Journal of Food Science*, *54(4)*, 997–1002.
579 Toribio, J. L., & Lozano, J. E. (1986). Heat induced browning of clarified apple juice at
580 high temperatures. *Journal of Food Science*, *51(1)*, 172–175.
581 Vallet-Regí, M., Balas, F., & Arcos, D. (2007). Mesoporous materials for drug delivery.
582 *Angewandte Chemie International Edition*, *46(40)*, 7548–7558.
583 Whitaker, J. R., & Lee, C. Y. (1995). Recent advances in chemistry of enzymatic
584 browning. In C. Y. Lee, & J. R. Whitaker (Eds.), *Enzymatic Browning and Its Prevention*
585 (pp. 2–7). ACS Symposium Series
586 Williams, D. C, Lim, M. H., Chen, A. O., Pangborn, R. M., & Whitaker, J. R. (1986). *Food*
587 *technology, 40*, 130-140
588
589
590

TABLE CAPTIONS

Table 1: Textural properties and organic content of the different silica matrix as-made, calcined and functionalised: UVM-7, MCM-41 nano, MCM-41 micro and Aerosil 200.

Table 2: Tyrosinase from the mushroom kinetics parameters (93,75U) in the presence of different substrates (Dopamine, L-tyrosine and chlorogenic acid) at different pHs and in the presence of 1mg of UVM-7-SH.

FIGURE CAPTIONS

Figure 1. Percentage of enzymatic activity inhibition after a 1-hour reaction at an enzyme concentration of 0.14 mg/mL and in the presence of 1 mg/mL of the material. Orange: calcined material; blue: thiol-functionalised materials

Figure 2. Percentage of immobilisation of enzymatic activity after a 1-hour reaction at an enzyme concentration of 0.14 mg/mL and in the presence of 1 mg/mL of the material. Orange: calcined material; blue: thiol-functionalised materials

Figure 3. Influence of the material concentration and pH on the enzymatic browning reaction using dopamine 0,12mM as a substrate after a one-hour reaction. Orange: pH 4.5; blue: pH 5.5

Figure 4. Colour evolution in an apple smoothie. (a) Golden Delicious without the material (left) and in the presence of 10 mg/mL of UVM-7-SH (right). (b) Granny Smith without the material (left) and in the presence of 10 mg/mL f UVM-7-SH (right). (c) Golden Delicious in the presence of 10 mg/mL of UVM-7-SH filtered after 5 minutes and stored at 4^{o}C (d) Golden Delicious in the presence of 10 mg/mL of UVM-7-SH filtered after 5 minutes and stored at room temperature

Table 1

Material		Area [a] (m^2g^{-1})	Mesopore volume [b] (cm^3g^{-1})	Mesopore diameter [b] (nm)	Textural pore diameter [b] (nm)	Textural pore volume [b] (cm^3g^{-1})	mmol SH/g SiO_2
UVM-7	calcined	866.8	0.66	2.69	41.3	1.02	-
	-SH	842.7	0.64	2.58	36.4	0.80	0.55
MCM-41 nano	calcined	1029.9	0.81	2.56	14.0	0.12	-
	-SH	902.8	0.55	2.48	14.2	0.11	0.78
MCM-41 micro	calcined	1030.7	0.67	2.38	-	-	-
	-SH	1035.5	0.74	2.36	-	-	0.56
Aerosil	calcined	195.9	-	-	14.9	0.25	-
	-SH	181.8	-	-	17.3	0.34	0.32

[a] BET specific surface calculated from the N2 adsorption-desorption isotherms.

[b] Pore volumes and pore size (diameter) calculated from the N_2 adsorption-desorption isotherms for the selected materials.

627 **Table 2**

628

Substrate	K_m[a](mM)	V_{max}[b] ($\Delta Abs_{420} min^{-1}$)	K_{cat}[c](ΔAbs_{420} mM^{-1} min^{-1})	Specific constant[d] (ΔAbs_{420} min^{-1} $(mM^2)^{-1}$)
Chlorogenic acid pH 5.5	0.31 ± 0.02	0.201 ± 0.006	1000 ± 30	3400 ± 100
L-tyrosine pH 5.5	0.19 ± 0.07	0.050 ± 0.007	260 ± 40	1500 ± 400
Dopamine pH 5.5	1.0 ± 0.2*	0.78 ± 0.09	3800 ± 500	3800 ± 400
Dopamine pH 4.5	0.87 ± 0.17*+	0.43 ± 0.07	2200 ± 300	2500 ± 100
Dopamine pH 3.5	0.5 ± 0.3*	0.0041 ± 0.0012	21 ± 6	40 ± 20
Dopamine + UVM-7-SH pH 4.5	1.0 ± 0.6+	0.009 ± 0.004	40 ± 20	44 ± 6

629 [a] Michaelis-Menten constant, dependent on enzyme concentration.
630 [b] Reaction rate, dependent on enzyme concentration.
631 [c] Catalytic constant, $K_{cat}=V_{max}/[E]$
632 [d] Specific constant, calculated by K_{cat}/K_m
633 * There are no statistically significant differences for $p < 0.05$ for the K_m constant at different pH.
634 + There are no statistically significant differences for $p < 0.05$ between K_m from dopamine at pH 4.5 in theabsence
635 and presence of UVM-7-SH.
636
637

Figure 1.

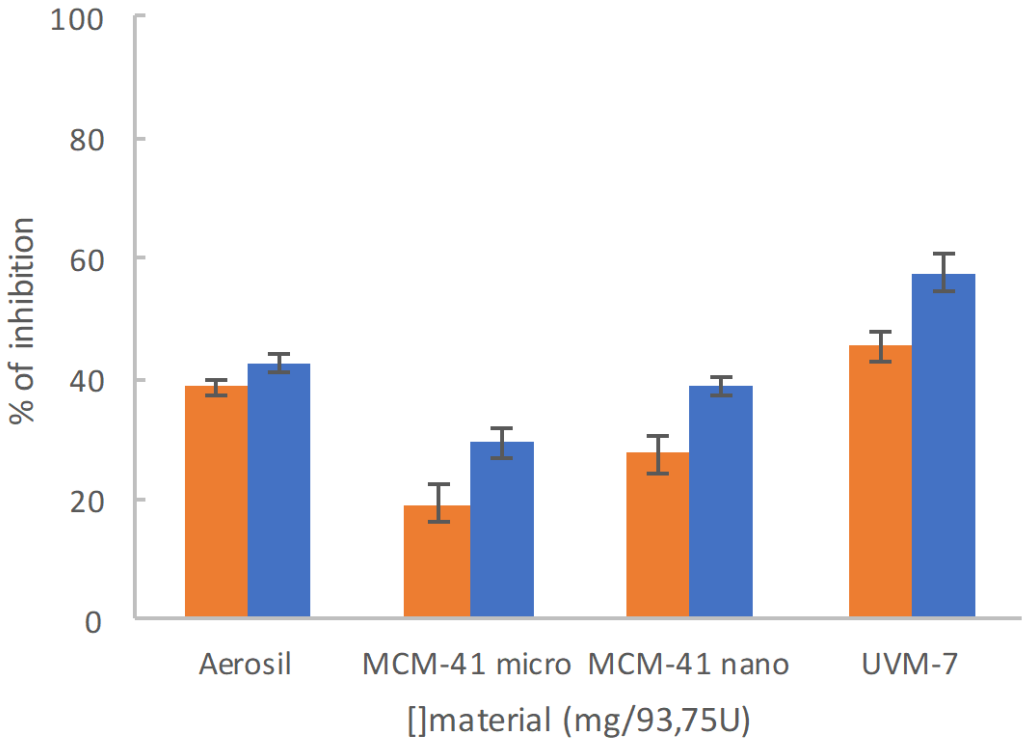
100
80
60
40
20
0
% of inhibition
Aerosil
MCM-41 micro
MCM-41 nano
UVM-7
[]material (mg/93,75U)

Figure 2

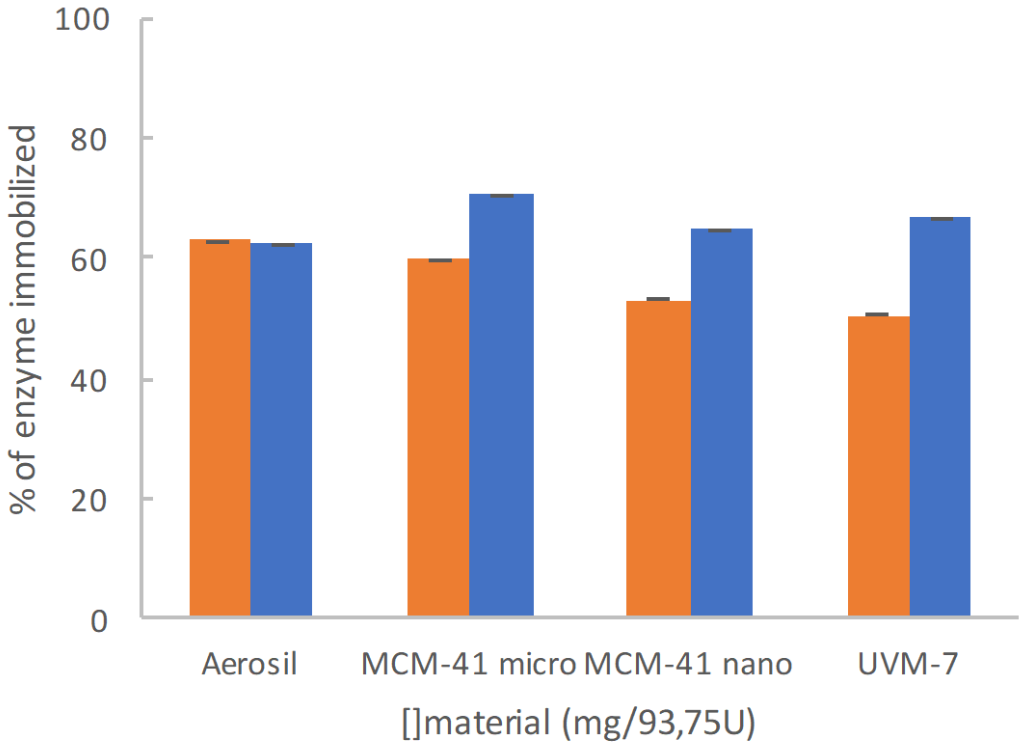
100
80
60
40
20
0
% of enzyme immobilized
Aerosil
MCM-41 micro
MCM-41 nano
UVM-7
[]material (mg/93,75U)

649 **Figure 3**

650

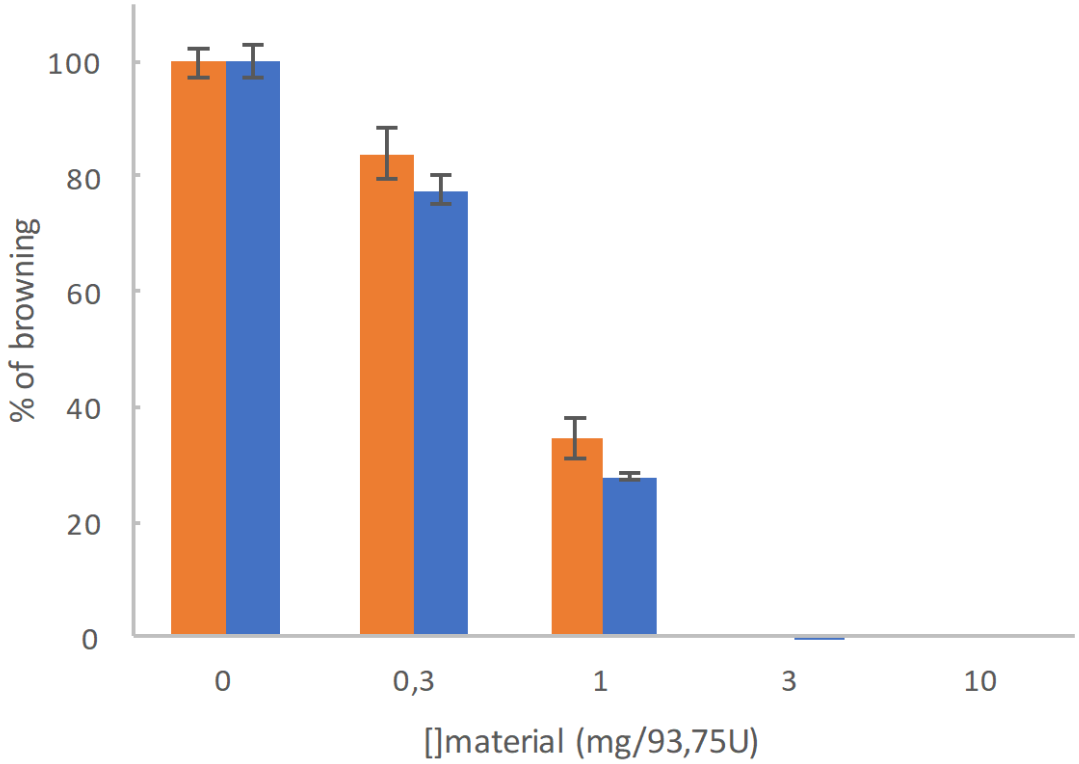

651

652

Figure 4

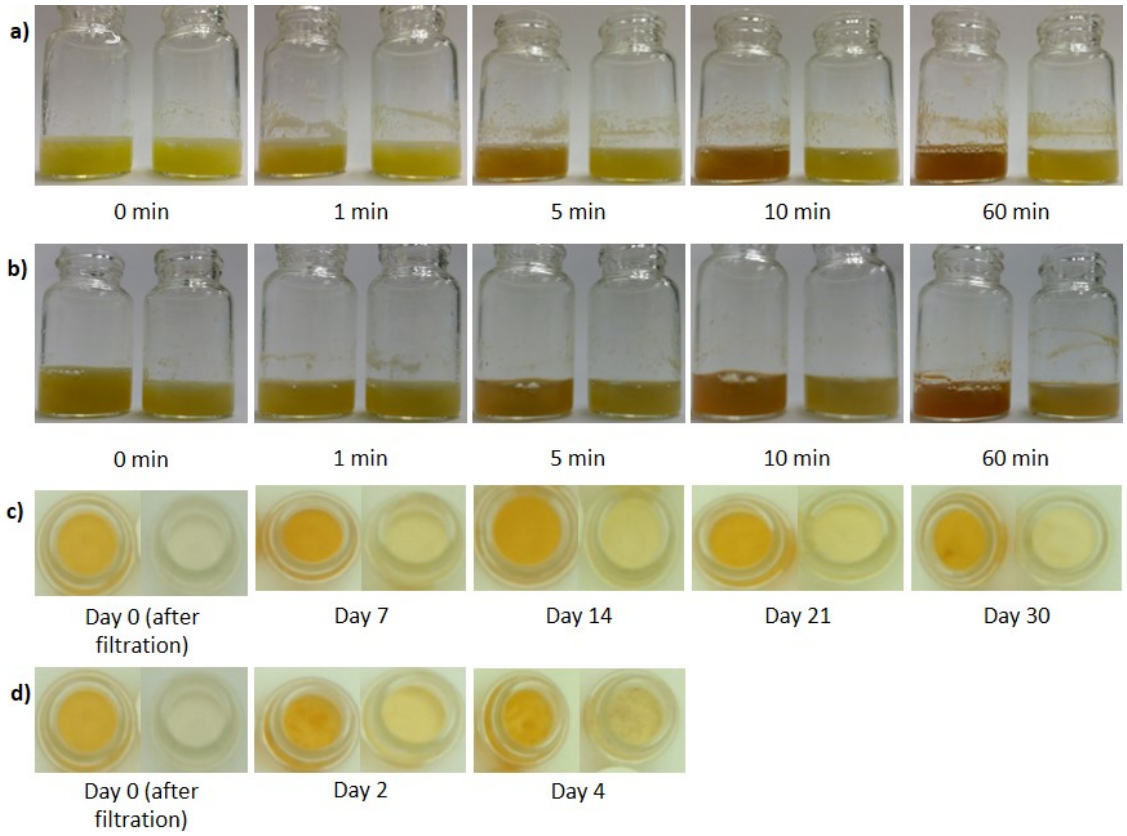
a)
0 min
1 min
5 min
10 min
60 min
b)
0 min
1 min
5 min
10 min
60 min
c)
Day 0 (after filtration)
Day 7
Day 14
Day 21
Day 30
d)
Day 0 (after filtration)
Day 2
Day 4